pubs.acs.org/acschemicalbiology

Articles

Discovery of Non-Cysteine-Targeting Covalent Inhibitors by Activity-Based Proteomic Screening with a Cysteine-Reactive Probe

Yejin Jung, Naotaka Noda, Junichiro Takaya, Masahiro Abo, Kohei Toh, Ken Tajiri, Changyi Cui, Lu Zhou, Shin-ichi Sato, and Motonari Uesugi*

Cite This: https://doi.org/10.1021/acschembio.1c00824

Read Online

ACCESS | Metrics & More | Article Recommendations | Supporting Information

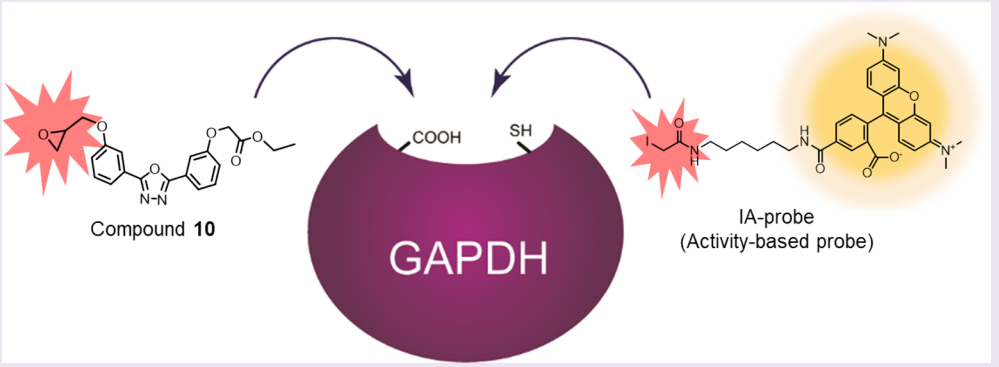

ABSTRACT: Covalent inhibitors of enzymes are increasingly appreciated as pharmaceutical seeds, yet discovering non-cysteine-targeting inhibitors remains challenging. Herein, we report an intriguing experience during our activity-based proteomic screening of 1601 reactive small molecules, in which we monitored the ability of library molecules to compete with a cysteine-reactive iodoacetamide probe. One epoxide molecule, F8, exhibited unexpected enhancement of the probe reactivity for glyceraldehyde-3-phosphate dehydrogenase (GAPDH), a rate-limiting glycolysis enzyme. In-depth mechanistic analysis suggests that F8 forms a covalent adduct with an aspartic acid in the active site to displace NAD^+, a cofactor of the enzyme, with concomitant enhancement of the probe reaction with the catalytic cysteine. The mechanistic underpinning permitted the identification of an optimized aspartate-reactive GAPDH inhibitor. Our findings exemplify that activity-based proteomic screening with a cysteine-reactive probe can be used for discovering covalent inhibitors that react with non-cysteine residues.

Small-molecule pharmaceuticals that form covalent bonds with their targets have historically been avoided due to misconceived concerns including off-target toxicity and potential immune responses. However, after the recent FDA approval of the rationally designed covalent drugs and the appreciation of covalent mechanisms of existing drugs, there has been increasing interest in discovering and designing covalently reacting bioactive molecules.[1−4] Covalent inhibitors offer potential benefits over classical non-covalent counterparts: prolonged duration of action, improved ligand efficiency, drug resistance evasion when the amino acids required for the catalysis of enzymes are targeted, and high selectivity when non-conserved amino acids are targeted.[1−8] The most popular approach to designing covalent inhibitors has been the incorporation of an electrophilic group into a non-covalent inhibitor.[7,9−12] However, discovering brand-new covalent inhibitors, in particular those targeting non-cysteine residues, remains challenging.[2,13,14]

New covalent inhibitors can be discovered by exploiting the chemoproteomic profiling of a chemical library of mild electrophile molecules. Such chemical library screenings have been performed with a purified protein,[15−21] in a cell-lysate proteome,[22−26] or in a cellular phenotypic context.[27−29] Small-scale screenings were also performed primarily by Cravatt and co-workers with reversible covalent fragments called "scout molecules".[23,26,30−32] Herein, we report an intriguing experience during our activity-based proteomic screening of 1601 electrophilic molecules against the cell-lysate proteome, which led to the discovery of non-cysteine-targeting inhibitors with a cysteine-reactive probe.

RESULTS AND DISCUSSION

Chemoproteomic Screening of 1601 Electrophilic Molecules. Each molecule in our collection of electrophilic

Received: October 18, 2021
Accepted: January 14, 2022

molecules is equipped with either chloroacetyl or epoxide groups. Chloroacetyl compounds, which react mostly with cysteines, have extensively been used for discovering and designing covalent probes. Epoxides, whose mild reactivity arises from their electrophilic nature and ring strain, react with nucleophilic amino acids, in particular cysteines, undergoing ring-opening.[33] In constructing the library, the molecular weights of the library members were maintained over 300 in order to increase the chances of selective interactions with proteins. Our electrophile-molecule library contains 1601 compounds (351 epoxides and 1250 chloroacetyls) and has previously been used for the discovery of a highly potent and selective covalent TRPA1 agonist.[34]

We screened the library for compounds that covalently react with any particular proteins in the proteome of human cells. The workflow of the screening is shown in Figure 1A. To

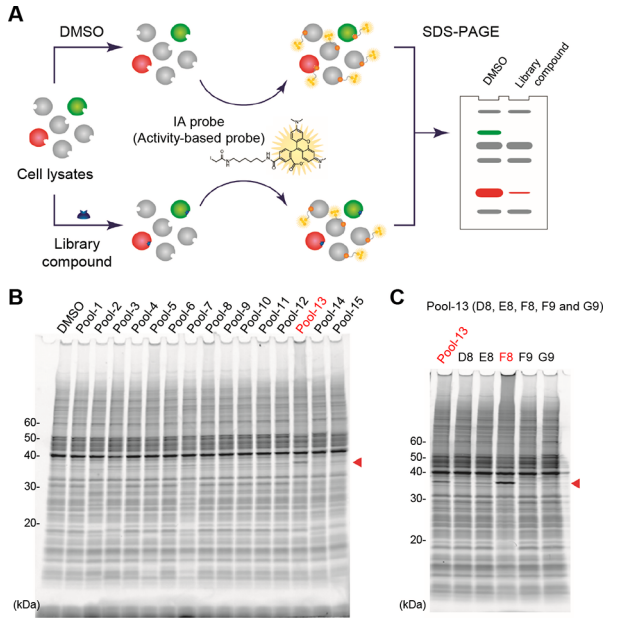

Figure 1. Chemoproteomic screening. (A) Workflow of the screening. HEK293 cell lysates were pretreated with each test pool for 60 min (chloroacetyl) or 4 h (epoxide) followed by treatment with an iodoacetamide-based probe for 1 h (IA probe, 1 μM). The samples were separated by SDS-PAGE and visualized by in-gel fluorescence scanning. (B) Typical fluorescence scanning image of the screening results (pools 1−15). HEK293 cell lysates were treated with either DMSO or 50 μM of library compound pools for 4 h before the treatment with a 1 μM IA probe for 1 h. A hit pool (pool-13) is highlighted in red, and an extra fluorescent band is indicated by a red arrowhead. (C) Deconvolution of pool-13. Each molecule in pool-13 was individually analyzed.

speed up the screening process, five compounds from the library were randomly combined giving a total of 379 test pools. Proteomic lysates of HEK293 cells were pretreated with each test pool for 60 min (chloroacetyl) or 4 h (epoxide) followed by treatment with an iodoacetamide-based probe for 1 h (IA probe, 1 μM). The IA probe (Figure 1A) that we used was a conjugate of TAMRA for fluorescence detection with iodoacetamide, which is usually more reactive than epoxide and chloroacetyl compounds and displays broad reactivity with proteins with reactive cysteines. The samples were separated by SDS-PAGE and visualized by in-gel fluorescence scanning. In this context, a compound that reacts with an IA probe-reactive protein will compete with the probe, resulting in the loss or decrease in fluorescence labeling of the protein in the gel profile. To reduce promiscuous, non-selective covalent reactions, the primary screening was performed at 1−10 μM.

The screening yielded multiple test pools that decreased selective bands in the fluorescence-scanned gels. Deconvolution of the test pool by examining the competition profile of the individual compounds identified a set of compound-band pairs. Proteins corresponding to the bands were purified by avidin agarose resins after using a biotin-conjugated IA probe instead of the fluorescent IA probe. Mass spectrometric sequencing of the decreased bands suggested that a majority of these compounds are likely to react with the enzymes that have already been documented in the literature to be targeted by reactive inhibitors, including the V-type proton ATPase catalytic subunit A,[28,35] heat shock protein 90,[36] aldehyde dehydrogenase,[37] eukaryotic translation initiation factor 4A,[38] and protein disulfide isomerase.[39] Furthermore, during the course of our study, Gygi and co-workers developed highly sensitive mass spectrometry-based screening methods using similar IA probes,[24] and such screenings of fragment libraries of chloroacetamide- or acrylamide-containing molecules permitted the identification of compounds that selectively react with a myriad of proteins. Given that our gel-based protein profiling is less sensitive than the mass spectrometry-based profiling, we decided not to pursue the same direction. Instead, we focused on an unexpected observation that we encountered during our gel-based screening.

Discovery of F8. Among the 379 pools tested, we noted one test pool of epoxides that showed an unexpected pattern of fluorescent bands on a gel: when the lysate was treated with the test pool, a new fluorescent band appeared around 40 kDa (Figure 1B). Such an appearance of a new band suggests that the covalent reaction of the test pool stimulates the reactivity of the IA probe with the protein corresponding to the bands. Deconvolution of the test pool by examining the competition profile of the individual compounds identified an epoxide compound, F8, to be responsible for the observed enhancement (Figure 1C). Intrigued by this unique finding, we selected this compound for more in-depth characterization.

The molecule F8 (Figure 2A) exhibited a dose-dependent increase in the probe labeling of the 40 kDa protein (Figure 2B). A silver-stained SDS-PAGE gel of the samples revealed a set of two newly appeared bands and a decreased band around 40 kDa (Figure 2C). We interpreted these data to reason that the treatment with F8 and the IA probe converted the decreased band (blue) to the slower migrating two bands (green and red), which may represent an F8-modified protein and a protein doubly modified by the IA probe and F8. In fact, when the cell lysates were treated with F8 alone, the decreased band (blue) was converted to a single slower migrating band (green). Addition of the IA probe to the sample further converted the band (green) to an even slower migrating band (red) whose electrophoretic mobility is consistent with that of the IA probe-reacted fluorescent band in in-gel fluorescence scanning (Figure 2C). We excised these bands for MS-based microsequencing and found that all the bands correspond to glyceraldehyde-3-phosphate dehydrogenase (GAPDH). GAPDH is a key glycolytic enzyme that catalyzes the conversion of glyceraldehyde-3-phosphate (G3P) into 1, 3-bisphosphoglycerate, with the parallel reduction of nicotinamide adenine dinucleotide (NAD^+) to NADH. Due to its pivotal role in glycolysis, GAPDH represents a rate-limiting

https://doi.org/10.1021/acschembio.1c00824
ACS Chem. Biol. XXXX, XXX, XXX−XXX

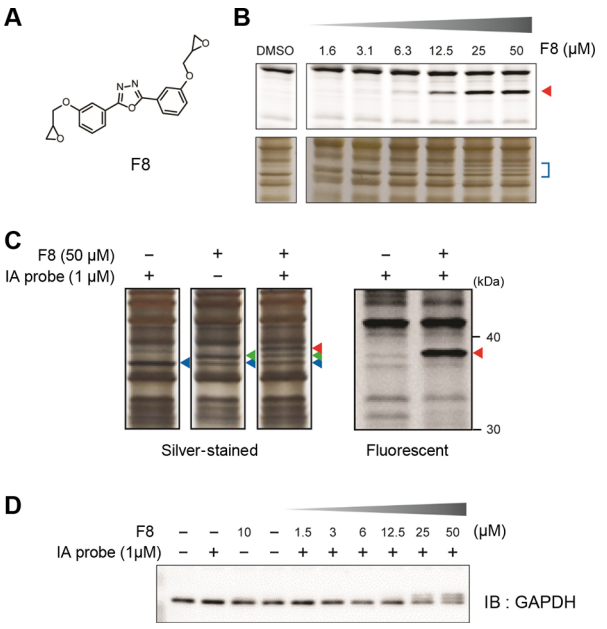

Figure 2. Effects of F8 on GAPDH band shifts. (A) Chemical structure of F8 (molecule **1**). (B) Dose-dependent effects of F8. HEK293 cell lysates were treated with various concentrations of F8 for 4 h followed by a 1 h treatment with a 1 μM IA probe. The samples were resolved by SDS-PAGE and visualized by fluorescence scanning (upper panel) and by silver staining (lower panel). (C) Expanded images of the silver-stained extra bands (left panel) and fluorescent bands (right panel). Bands for unmodified, F8-modified, and F8+IA probe-modified bands are indicated by blue, green, and red arrowheads, respectively. (D) Western blotting analysis of GAPDH. HEK293 cell lysates were treated with various concentrations of F8 for 4 h followed by a 1 h treatment with a 1 μM IA probe.

enzyme in those cells that mostly rely on glycolysis for energy production. In this regard, GAPDH inhibition can be a valuable approach for the development of anticancer,[40−42] immunomodulatory,[43−46] antibacterial,[47] Alzheimer's disease,[48] and antiparasitic drugs.[49,50]

In order to corroborate the protein identity, we conducted Western blotting analysis of cell lysates treated with F8 and/or the IA probe, using an anti-GAPDH antibody (Figure 2D). Treatment with 10 μM F8 alone displayed a faint band slightly upper shifted from that of GAPDH, while the IA probe alone displayed no detectable band shift. The cell lysates treated with both F8 and the IA probe displayed two slower migrating bands in the Western blots, as observed on the silver-stained gel.

For further validation, we transiently expressed FLAG-tagged GAPDH in HEK293 cells to assess covalent adduct formation with F8 in the presence or absence of the IA probe by SDS-PAGE and in-gel fluorescence scanning (Figure 3). In the presence of F8, the cell lysates containing FLAG-GAPDH displayed an additional fluorescent band (blue) whose molecular weight is higher than that of endogenous GAPDH (red). Western blotting analysis of the samples with an anti-FLAG antibody showed a slight band shift of FLAG-GAPDH in the presence of F8, which was further pronounced by adding the IA probe to the samples (Figure 3). These results collectively indicate that F8 covalently reacts with GAPDH and thereby stimulates the subsequent covalent reaction with the IA probe.

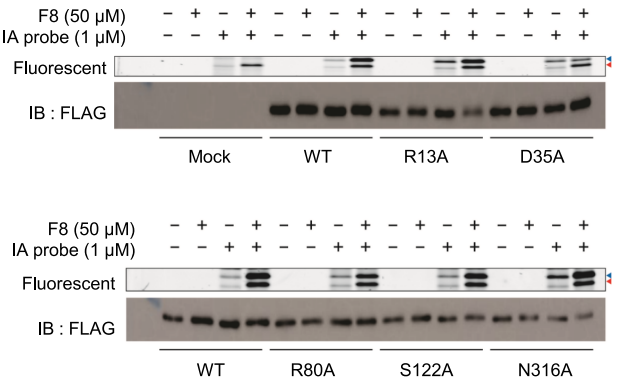

Figure 3. Effects of F8 on GAPDH point mutants. The FLAG-tagged wild type (WT) or mutants of GAPDH (R13A, D35A, R80A, S122A, and N316A) were transiently expressed in HEK293 cells. The cell lysates were treated with 50 μM F8 for 4 h followed by a 1 h treatment with the IA probe (1 μM). The samples were resolved by SDS-PAGE and visualized by fluorescence scanning and FLAG Western blotting. Endogenous GAPDH and FLAG-tagged GAPDH are indicated by red and blue arrowheads, respectively.

Analysis of Underlying Mechanisms. Human GAPDH harbors three cysteine residues (C152, C156, and C247), of which only C152 has catalytic activity. In light of the general trend of epoxides and IA for cysteine modification, we expected that F8 and the IA probe would react with cysteines on GAPDH. To deconvolute the engagement of the cysteines, we prepared HEK293 cells transiently expressing FLAG-tagged GAPDH or its cysteine-to-alanine mutants. Lysates of the cells were incubated for 4 h with F8 or a vehicle control. Covalent adduct formation was assessed by SDS-PAGE and blotting with an anti-FLAG antibody. As shown in Figure S1, the band of FLAG-GAPDH was slightly shifted by incubation with increasing amounts of F8. Similar band shifts were observed in all the cysteine mutants that we tested (C152A, C156A, and C247A), suggesting that F8 does not covalently react with any of these cysteines at detectable levels. To examine whether these F8 adducts of the GAPDH mutants enhance the subsequent reactivity with the IA probe, we added the IA probe to the F8-treated lysates and analyzed the resulting IA adducts by in-gel fluorescence scanning (Figure S1). The cell lysates with FLAG-GAPDH displayed a strong fluorescent band (blue) migrating slower than that of endogenous GAPDH (red) on an SDS-PAGE gel. This extra band disappeared when C152 was mutated with alanine (C152A), while cell lysates containing each of the other two cysteine mutants (C156A and C247A) maintained the extra band. Overall, these results suggest that F8 covalently reacts with a non-cysteine residue to stimulate the subsequent reaction of Cys152 with the IA probe.

To identify nucleophilic amino acids that F8 reacts with, we performed mutational studies in which an array of nucleophilic amino acids in the enzyme active site were replaced by alanine. Cell lysates of HEK293 cells transiently expressing FLAG-tagged GAPDH or its mutants were incubated for 4 h with F8 in the presence or absence of the IA probe. As shown in Figure 3, the mutation of Asp35 to Ala abolished both the adduct formation and the enhanced IA probe activity of F8. In contrast, the other FLAG-GAPDH mutants maintained the F8-induced shifts of the Western blotting bands and the subsequent enhanced reactivity of the IA probe. These results

https://doi.org/10.1021/acschembio.1c00824
ACS Chem. Biol. XXXX, XXX, XXX−XXX

suggest that F8 covalently reacts with Asp35 to stimulate the subsequent reaction of Cys152 with the IA probe.

How the covalent reaction of F8 with Asp35 potentiates the reactivity of the IA probe to Cys152 remains unclear. Asp35 is located in the opposite edge of the active site of GAPDH where its side chain forms hydrogen bonds with the ribose hydroxy groups of NAD^+, the cofactor of GAPDH. Indeed, addition of excess amounts of NAD^+ to the cell lysates reduced the formation of F8-GAPDH adducts as evidenced by the band shifts of endogenous GAPDH in a silver-stained gel (Figure S2). In contrast, addition of G3P, a substrate of GAPDH, had no detectable effects. We postulate that the covalent reaction of F8, which is smaller than NAD^+, with Asp35 may displace NAD^+ to make the active site less crowded, thereby increasing the accessibility of Cys152 for the reaction with the IA probe.

Structure−Activity Relationship of F8 Analogues. The molecule F8 is equipped with two epoxide groups. To examine the importance of these two warheads in the covalent bond formation, we set out to analyze the reactivity of three F8 analogues (molecules **2**−**4**) with GAPDH in cell lysates (Figure 4A,B and Figure S3). The removal of both epoxide groups (molecule **2**) completely impaired the ability of F8 to react with GAPDH, as confirmed by band shifts. In contrast, the molecule **3**, which carries a single epoxide group, exhibited an upper band shift of GAPDH, retaining its reactivity to GAPDH. Approximately, twice more concentrations of the molecule **3** were needed to achieve the reaction levels of F8, possibly due to the 50% net concentrations of epoxide functional groups in the molecule **3** samples (Figure S3). Similar results were obtained for their ability to enhance the reactivity of the IA probe to GAPDH and FLAG-GAPDH. These results indicate that at least one epoxide group is required for the observed covalent adduct formation and enhanced probe reactivity with GAPDH.

During the structure−activity relationship studies of F8, we noticed the importance of the benzene group for the reaction with GAPDH: the removal of a benzene group from the molecule **3** (molecule **4**) abolished its reactivity to GAPDH as confirmed by the band shift on an SDS-PAGE gel and the IA probe reactivity (Figure 4B). We therefore introduced a suite of drug-like functional groups to the benzene moiety with the expectation of a higher activity to GAPDH. The resulting six analogues of F8 (molecules **5**−**10**) were examined for their ability to form adducts with GAPDH with concomitant activation of the IA probe in cell lysates. As shown in Figure 4B, three analogues (**5**, **8**, and **10**) exhibited a more potent activity in enhancing the reactivity of the IA probe than that of F8. A similar trend was observed for overexpressed FLAG-GAPDH. Mutation of Asp35 to Ala in FLAG-GAPDH completely abolished their activity to the overexpressed GAPDH, while their activity to endogenous GAPDH remained (Figure 4C).

To confirm the covalent adduct formation of the F8 analogues with Asp35, the upper shifted band of endogenous GAPDH was excised from the silver-stained SDS-PAGE gels and trypsinized for liquid chromatography−tandem MS (LC−MS/MS) analysis. Although the samples of F8 and **10** failed to yield MS-detectable adduct peptides, the sample of the molecule **8**, a dimethylamino derivative of F8, displayed an MS-detectable Asp35-adduct peptide (amino acids 28−55; Figure 5), presumably due to the enhanced ionization of its dimethylamino group. No other **8** adducts were detected,

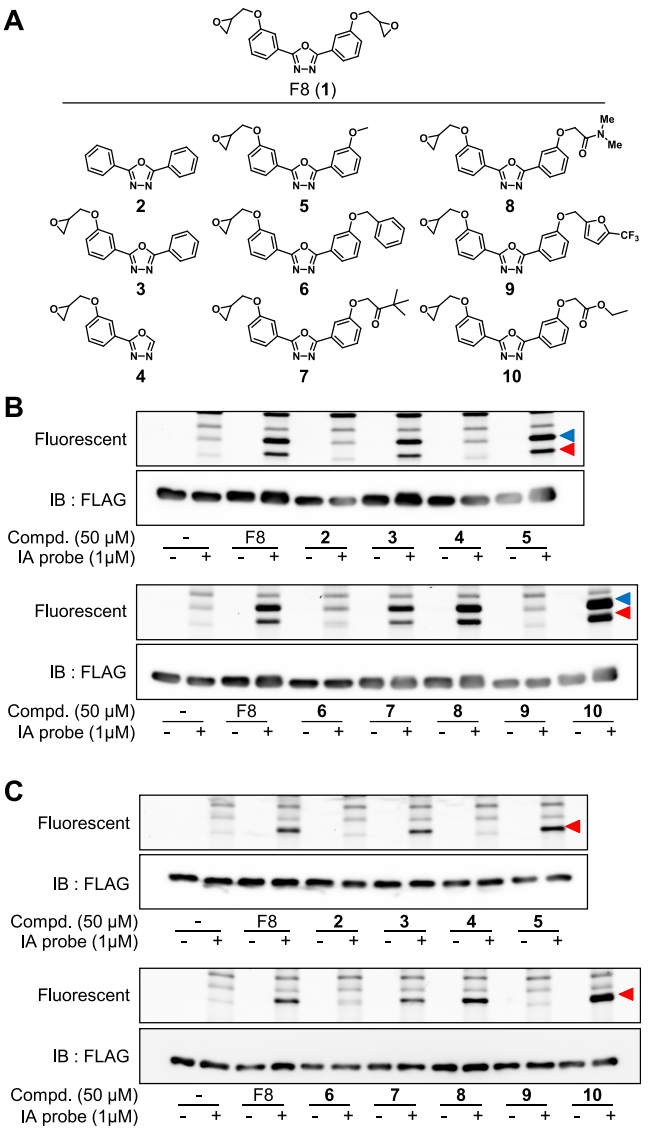

Figure 4. F8 analogues and their ability to form covalent adducts with GAPDH. (A) Chemical structures of F8 analogues **2**−**10**. (B) Modification of FLAG-tagged GAPDH (wild-type). Lysates of HEK293 cells expressing FLAG-tagged GAPDH (wild-type) were treated with 50 μM F8 or its analogues for 4 h followed by a 1 h treatment with a 1 μM IA probe. The samples were resolved by SDS-PAGE and visualized by fluorescence scanning (upper panel) or Western blotting with a FLAG antibody (lower panel). Positions of endogenous GAPDH and FLAG-tagged GAPDH are indicated by red and blue arrowheads, respectively. (C) Effects on the FLAG-tagged GAPDH D35A mutant. The experiments were performed as in (B).

indicating that the molecule **8** covalently reacted selectively with Asp35.

To gain insights into the selectivity of the F8 analogues, we compared the competition profiling of molecules F8, **5**, **8**, **10**, and **2** (Figure S4). In the lane of F8, several protein bands are missing compared with the control lane, indicating that F8 reacts with proteins other than GAPDH (indicated by blue arrowheads). These bands were partially restored in the lanes of **5** and **10**. Although the identities of the bands remain unknown, the results suggest that molecules **5** and **10** may be more selective than F8.

Encouraged by the cell-lysate results, we next sought to characterize the cellular engagement of the F8 analogues

https://doi.org/10.1021/acschembio.1c00824
ACS Chem. Biol. XXXX, XXX, XXX−XXX

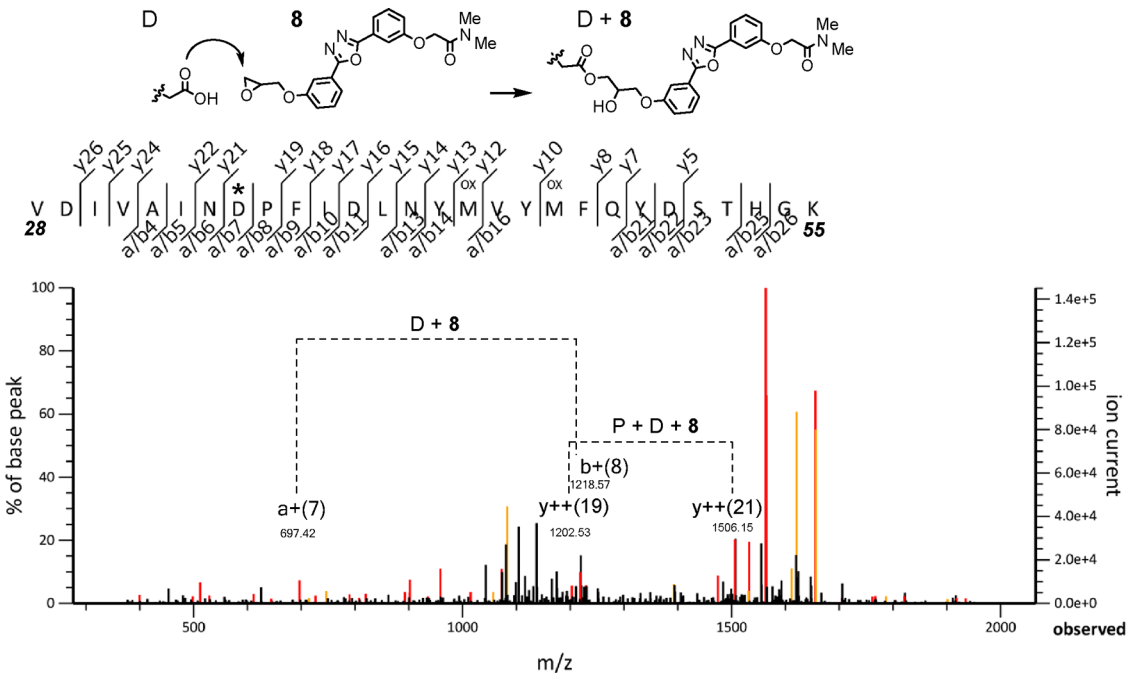

Figure 5. LC−MS/MS spectrum of a molecule **8**-modified GAPDH peptide (amino acids 28−55). The sequence and detected fragments of the peptide are shown. HEK293 cell lysates were treated with 50 μM **8** for 24 h and separated by SDS-PAGE. The shifted GAPDH band was excised and digested in-gel by trypsin for subsequent LC−MS/MS analysis. Sequence-matched peaks are highlighted in red and yellow.

(Figure S5). As observed in cell lysates, the IA probe alone displayed little reactivity to GAPDH in live cells. Although F8 potentiated the probe reaction with GAPDH, its ability to do so in cells was less than that in cell lysates. Among the three F8 analogues, the molecule **10** showed the most potent ability to enhance the probe reactivity in cells, while the molecule **2**, which lacks epoxide groups, displayed no detectable enhancement.

Molecule 10 as a Covalent GAPDH Inhibitor. We next assessed the impacts of F8 analogues on the enzymatic activity of GAPDH. Our initial expectation was that they would potentiate GAPDH enzyme activity through activation of the catalytic cysteine Cys152. However, later studies, as shown earlier, indicated that they form covalent adducts with Asp35, which directly contacts NAD^+, suggesting that these F8 analogues inhibit the enzymatic activity of GAPDH by competing with the cofactor. In fact, F8, **8**, and **10** displayed a concentration-dependent inactivation of GAPDH in cell lysates, while the molecule **2**, which lacks epoxide groups, displayed no detectable inhibition (Figure 6A). The same samples were also analyzed by silver-stained SDS-PAGE (Figure 6B). The extents of band shifts were paralleled with the enzyme inhibition. For example, a 50 μM molecule **10** displayed an almost complete shift of the GAPDH band.

We compared the GAPDH inhibitory activity of the F8 analogues with that of koningic acid, a known GAPDH inhibitor containing an epoxide group, and found that the ability of koningic acid to inhibit the enzymatic activity of GAPDH was approximately 1000 times more potent (IC_{50} = 60.4 nM) than those of the F8 analogues (Figure S6A). However, koningic acid failed to enhance the reactivity of the IA probe, suggesting that the mode of action is distinct (Figure S6B).

We next assessed the cellular activity of the F8 analogues. Cell viability assays and lactate production assays in HEK293

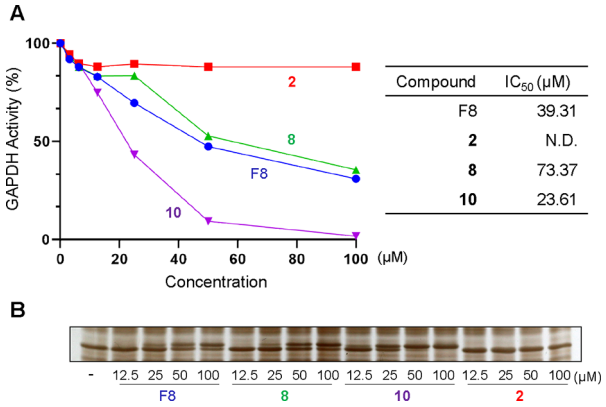

Figure 6. Inhibition of GAPDH enzymatic activity by F8 analogues. (A) HEK293 cell lysates were treated with 0, 3.125, 6.25, 12.5, 25, 50, and 100 μM F8, **2**, **8**, and **10** for 24 h before measurement of GAPDH activity as described in the Supporting Information. Calculated IC_{50} values are shown in the right panel. (B) Adduct status of GAPDH. The same enzyme assay samples were analyzed by SDS-PAGE and silver staining. N.D.: not determined.

cells showed IC_{50} values of F8, **2**, **8**, and **10** consistent with those of cell-lysate GAPDH inhibition (Figures S7 and S8). In both cellular assays, the molecule **10** displayed the most potent activity in line with its highest enhancement of the probe reactivity in cells (Figure S5).

An interesting property of F8 and its analogues is that, when purified GAPDH is used for similar biochemical experiments, they exhibit no enhancement of the IA probe reaction (Figure S9). This property hampered the in-depth biochemical analysis of the activity of F8 and its analogues with purified GAPDH. Perhaps, the status of GAPDH and its active site in cell lysates or live cells may be distinct from those in the purified enzyme, underscoring the importance of cell-lysate- or cell-based screening in discovering small-molecule GAPDH modulators.

https://doi.org/10.1021/acschembio.1c00824
ACS Chem. Biol. XXXX, XXX, XXX−XXX

CONCLUSIONS

A number of synthetic or naturally occurring epoxide-containing GAPDH inhibitors have been reported;[51] however, all of them have been proposed to react with the catalytic cysteine. Our activity-based proteomic screening of 1601 reactive small molecules led to the discovery of a new class of epoxide-containing GAPDH inhibitors that covalently react with an aspartate residue. Since the GAPDH inhibitory activities of our molecules remain modest, further structural optimization is needed to generate specific Asp-targeting GAPDH inhibitors.

Reactivity enhancement of an activity-based probe has recently been observed for the discovery of non-covalent activators of LYPLAL1, a metabolism-linked serine hydrolase. This compound in fact increased LYPLAL1 enzymatic activity in cells, suggesting that activity-based protein profiling aids in the discovery of enzyme activators.[52] Our experience described in the present study implies an additional utility of such probe activity enhancement as a guide: discovery of enzyme inhibitors that covalently react with non-catalytic residues. Close inspection of our screening data revealed a number of enhanced bands in the competition profiles of screening pools (examples are shown in Figure S10), indicating that enhancement of the probe reactivity occurs more frequently than what we imagined. Our case study on GAPDH exemplifies that activity-based proteomic screening with a cysteine-reactive probe can be used for discovering covalent inhibitors that react with non-cysteine residues.

METHODS

Chemical Library Screening. The reactive chemical library that we used for the screening is a collection of the compounds purchased from the following sources: AMRI Hungary, ASINEX, AnalytiCon Discovery, BIONET, Butt Park, Labotest, Life Chemicals, Peakdale, Princeton, MDD, OTAVA, Pharmeks, Enamine, Scientific Exchange, TOSLab, Vitas M, and TimTec. HEK293 cells were grown in a 100 mm dish until it reached a 90% confluency. The cells were collected into a 50 mL tube by scraping, washed twice with 1× PBS, and lysed in PBS by sonication. After centrifugation (15,000 rpm, 20 min, and 4 °C), an aliquot of the soluble fraction was dispensed onto a 96-well plate. Each well of the plate was treated with a chemical library pool (5 compounds/pool) that was added. The final concentrations of the compounds were 1 or 10 μM. After gentle shaking for 1 (chloroacetyl) or 4 h (epoxide) at 25 °C, the IA probe (1% DMSO) was added (1 μM) and incubated for 1 h at 25 °C. The reaction was stopped by adding 6× SDS-PAGE loading buffer (Nacalai Tesque). The proteins were resolved on 7.5 and 15% SDS-PAGE acrylamide gels (Super Sep Ace, Fujifilm), and their fluorescence images were obtained using a Typhoon FLA 9000 (GE Healthcare).

LC−MS/MS Analysis of GAPDH. HEK293 cell lysates were treated with 50 μM of each compound for 24 h at 25 °C. After incubation, samples were mixed with 6× SDS-PAGE loading buffer (Nacalai), resolved on a 12% SDS-PAGE gel, and visualized by silver staining (Silver Stain MS kit, Wako). The shifted GAPDH bands were excised and digested in-gel by trypsin. The peptide mixtures were then fractionated by C18 reverse-phase chromatography (3 μm, ID 0.075 mm × 150 mm, CERI). The peptides were eluted at a flow rate of 300 nL/min with a linear gradient of 0 to 90% with solvent B. The compositions of solvents A and B were 0.1% formic acid in water and 100% acetonitrile, respectively. The molecular masses of the resulting peptides were searched against the human amino acid sequence dataset (UniProt human proteome 20201007) using MASCOT version 2.6 (Matrix Science). Carbamidomethylation of cysteine was set as a fixed modification, and oxidation of methionine and acetylation of protein N-termini were included as variable modifications. Identified proteins were analyzed by Scaffold. We searched for peptides modified by F8 (+366.1216 Da), **8** (+395.1481 Da), and **10** (+396.1321 Da) on Cys, Asp, Ser, Asn, and Arg as well as oxidized Met (+15.9949 Da) and acetylation of N-termini (+42.0114 Da) as variable modifications.

See the Supporting Information for experimental details.

ASSOCIATED CONTENT

Supporting Information

The Supporting Information is available free of charge at https://pubs.acs.org/doi/10.1021/acschembio.1c00824.

Supporting figures, methods for experiments, LC−MS/MS data, chemical synthesis, and NMR and MS data (PDF)

AUTHOR INFORMATION

Corresponding Author

Motonari Uesugi − *Institute for Chemical Research and Institute for Integrated Cell-Material Sciences (WPI-iCeMS), Kyoto University, Uji, Kyoto 611-0011, Japan; School of Pharmacy, Fudan University, Shanghai 201203, China;* orcid.org/0000-0002-8515-445X; Email: uesugi@scl.kyoto-u.ac.jp

Authors

Yejin Jung − *Institute for Chemical Research, Kyoto University, Uji, Kyoto 611-0011, Japan; Graduate School of Medicine, Kyoto University, Kyoto 606-8501, Japan*

Naotaka Noda − *Institute for Chemical Research, Kyoto University, Uji, Kyoto 611-0011, Japan; Graduate School of Medicine, Kyoto University, Kyoto 606-8501, Japan*

Junichiro Takaya − *Institute for Chemical Research, Kyoto University, Uji, Kyoto 611-0011, Japan; Graduate School of Medicine, Kyoto University, Kyoto 606-8501, Japan*

Masahiro Abo − *Institute for Chemical Research, Kyoto University, Uji, Kyoto 611-0011, Japan*

Kohei Toh − *Institute for Chemical Research, Kyoto University, Uji, Kyoto 611-0011, Japan*

Ken Tajiri − *Institute for Chemical Research, Kyoto University, Uji, Kyoto 611-0011, Japan*

Changyi Cui − *School of Pharmacy, Fudan University, Shanghai 201203, China*

Lu Zhou − *School of Pharmacy, Fudan University, Shanghai 201203, China;* orcid.org/0000-0002-6807-2647

Shin-ichi Sato − *Institute for Chemical Research, Kyoto University, Uji, Kyoto 611-0011, Japan;* orcid.org/0000-0003-3085-419X

Complete contact information is available at: https://pubs.acs.org/10.1021/acschembio.1c00824

Author Contributions

Y.J. conducted the screening and biochemical experiments. J.T. contributed to the initial analysis of F8. N.N., K.Toh, and K.Tajiri synthesized the chemicals. S.S. provided advice on data curation and designed the figures. M.A., C.C., and L.Z. discussed the data. M.U. supervised the project and participated in planning the experiment and writing the manuscript.

Notes

The authors declare no competing financial interest.

https://doi.org/10.1021/acschembio.1c00824
ACS Chem. Biol. XXXX, XXX, XXX−XXX

■ ACKNOWLEDGMENTS

This work was supported by JSPS (19H00922 and 17H06408 to M.U.), the Kobayashi Foundation, and SPIRITS2019 of the Kyoto University. Y.J. was supported by Kobayashi Foundation Fellowship. The authors thank T. Morii and E. Nakata (Kyoto University) for access to their equipment and K. Lee (Ewha Woman's University) for sharing GAPDH plasmid constructs. This work was inspired by the international and interdisciplinary environments of WPI-iCeMS, the JSPS A3 Foresight Program "Asian Chemical Probe Research Hub," and the JSPS CORE-to-CORE Program "Asian Chemical Biology Initiative."

■ ABBREVIATIONS

GAPDH, glyceraldehyde-3-phosphate dehydrogenase; NAD^+, nicotinamide adenine dinucleotide; NADH, nicotinamide adenine dinucleotide (NAD) + hydrogen (H); FDA, Food and Drug Administration; TRPA1, transient receptor potential cation channel, subfamily A, member 1; DMSO, dimethyl sulfoxide; IA, iodoacetamide; TAMRA, tetramethylrhodamine; SDS-PAGE, sodium dodecyl sulfate−polyacrylamide gel electrophoresis; G3P, glyceraldehyde 3-phosphate; LC−MS/MS, liquid chromatography with tandem mass spectrometry; LYPLAL1, lysophospholipase-like protein 1

■ REFERENCES

(1) Bauer, R. A. Covalent inhibitors in drug discovery: from accidental discoveries to avoided liabilities and designed therapies. *Drug Discovery Today* **2015**, *20*, 1061−1073.
(2) Singh, J.; Petter, R. C.; Baillie, T. A.; Whitty, A. The resurgence of covalent drugs. *Nat. Rev. Drug Discov.* **2011**, *10*, 307−317.
(3) Long, M. J. C.; Aye, Y. Privileged Electrophile Sensors: A Resource for Covalent Drug Development. *Cell Chem. Biol.* **2017**, *24*, 787−800.
(4) Zhang, T.; Hatcher, J. M.; Teng, M.; Gray, N. S.; Kostic, M. Recent Advances in Selective and Irreversible Covalent Ligand Development and Validation. *Cell Chem. Biol.* **2019**, *26*, 1486−1500.
(5) Barf, T.; Kaptein, A. Irreversible protein kinase inhibitors: balancing the benefits and risks. *J. Med. Chem.* **2012**, *55*, 6243−6262.
(6) Baillie, T. A. Targeted Covalent Inhibitors for Drug Design. *Angew. Chem. Int. Ed. Engl.* **2016**, *55*, 13408−13421.
(7) Cohen, M. S.; Zhang, C.; Shokat, K. M.; Taunton, J. Structural bioinformatics-based design of selective, irreversible kinase inhibitors. *Science* **2005**, *308*, 1318−1321.
(8) Bradshaw, J. M.; McFarland, J. M.; Paavilainen, V. O.; Bisconte, A.; Tam, D.; Phan, V. T.; Romanov, S.; Finkle, D.; Shu, J.; Patel, V.; et al. Prolonged and tunable residence time using reversible covalent kinase inhibitors. *Nat. Chem. Biol.* **2015**, *11*, 525−531.
(9) McAulay, K.; Hoyt, E. A.; Thomas, M.; Schimpl, M.; Bodnarchuk, M. S.; Lewis, H. J.; Barratt, D.; Bhavsar, D.; Robinson, D. M.; Deery, M. J.; et al. Alkynyl Benzoxazines and Dihydroquinazolines as Cysteine Targeting Covalent Warheads and Their Application in Identification of Selective Irreversible Kinase Inhibitors. *J. Am. Chem. Soc.* **2020**, *142*, 10358−10372.
(10) Matthews, D. A.; Dragovich, P. S.; Webber, S. E.; Fuhrman, S. A.; Patick, A. K.; Zalman, L. S.; Hendrickson, T. F.; Love, R. A.; Prins, T. J.; Marakovits, J. T.; et al. Structure-assisted design of mechanism-based irreversible inhibitors of human rhinovirus 3C protease with potent antiviral activity against multiple rhinovirus serotypes. *Proc. Natl. Acad. Sci. U. S. A.* **1999**, *96*, 11000−11007.
(11) Schnute, M. E.; Benoit, S. E.; Buchler, I. P.; Caspers, N.; Grapperhaus, M. L.; Han, S.; Hotchandani, R.; Huang, N.; Hughes, R. O.; Juba, B. M.; et al. Aminopyrazole Carboxamide Bruton's Tyrosine Kinase Inhibitors. Irreversible to Reversible Covalent Reactive Group Tuning. *ACS Med. Chem. Lett.* **2019**, *10*, 80−85.
(12) Zhou, W.; Hur, W.; McDermott, U.; Dutt, A.; Xian, W.; Ficarro, S. B.; Zhang, J.; Sharma, S. V.; Brugge, J.; Meyerson, M.; et al. A structure-guided approach to creating covalent FGFR inhibitors. *Chem. Biol.* **2010**, *17*, 285−295.
(13) Pettinger, J.; Jones, K.; Cheeseman, M. D. Lysine-Targeting Covalent Inhibitors. *Angew. Chem. Int. Ed. Engl.* **2017**, *56*, 15200−15209.
(14) Mukherjee, H.; Grimster, N. P. Beyond cysteine: recent developments in the area of targeted covalent inhibition. *Curr. Opin. Chem. Biol.* **2018**, *44*, 30−38.
(15) London, N.; Miller, R. M.; Krishnan, S.; Uchida, K.; Irwin, J. J.; Eidam, O.; Gibold, L.; Cimermančič, P.; Bonnet, R.; Shoichet, B. K.; Taunton, J. Covalent docking of large libraries for the discovery of chemical probes. *Nat. Chem. Biol.* **2014**, *10*, 1066−1072.
(16) Resnick, E.; Bradley, A.; Gan, J.; Douangamath, A.; Krojer, T.; Sethi, R.; Geurink, P. P.; Aimon, A.; Amitai, G.; Bellini, D.; Bennett, J.; Fairhead, M.; Fedorov, O.; Gabizon, R.; Gan, J.; et al. Rapid Covalent-Probe Discovery by Electrophile-Fragment Screening. *J. Am. Chem. Soc.* **2019**, *141*, 8951−8968.
(17) Boike, L.; Cioffi, A. G.; Majewski, F. C.; Co, J.; Henning, N. J.; Jones, M. D.; Liu, G.; McKenna, J. M.; Tallarico, J. A.; Schirle, M.; Nomura, D. K. Discovery of a Functional Covalent Ligand Targeting an Intrinsically Disordered Cysteine within MYC. *Cell Chem. Biol.* **2021**, *28*, 4.
(18) Dubiella, C.; Pinch, B. J.; Koikawa, K.; Zaidman, D.; Poon, E.; Manz, T. D.; Nabet, B.; He, S.; Resnick, E.; Rogel, A.; et al. Sulfopin is a covalent inhibitor of Pin1 that blocks Myc-driven tumors in vivo. *Nat. Chem. Biol.* **2021**, *17*, 954−963.
(19) Craven, G. B.; Affron, D. P.; Allen, C. E.; Matthies, S.; Greener, J. G.; Morgan, R. M. L.; Tate, E. W.; Armstrong, A.; Mann, D. J. High-Throughput Kinetic Analysis for Target-Directed Covalent Ligand Discovery. *Angew. Chem. Int. Ed. Engl.* **2018**, *57*, 5257−5261.
(20) Bachovchin, D. A.; Koblan, L. W.; Wu, W.; Liu, Y.; Li, Y.; Zhao, P.; Woznica, I.; Shu, Y.; Lai, J. H.; Poplawski, S. E.; et al. A high-throughput, multiplexed assay for superfamily-wide profiling of enzyme activity. *Nat. Chem. Biol.* **2014**, *10*, 656−663.
(21) Ostrem, J. M.; Peters, U.; Sos, M. L.; Wells, J. A.; Shokat, K. M. K-Ras(G12C) inhibitors allosterically control GTP affinity and effector interactions. *Nature* **2013**, *503*, 548−551.
(22) Banerjee, R.; Pace, N. J.; Brown, D. R.; Weerapana, E. 1,3,5-Triazine as a modular scaffold for covalent inhibitors with streamlined target identification. *J. Am. Chem. Soc.* **2013**, *135*, 2497−2500.
(23) Abbasov, M. E.; Kavanagh, M. E.; Ichu, T. A.; Lazear, M. R.; Tao, Y.; Crowley, V. M.; Am Ende, C. W.; Hacker, S. M.; Ho, J.; Dix, M. M.; Suciu, R.; Hayward, M. M.; Kiessling, L. L.; Cravatt, B. F. A proteome-wide atlas of lysine-reactive chemistry. *Nat. Chem.* **2021**, 1081.
(24) Kuljanin, M.; Mitchell, D. C.; Schweppe, D. K.; Gikandi, A. S.; Nusinow, D. P.; Bulloch, N. J.; Vinogradova, E. V.; Wilson, D. L.; Kool, E. T.; Mancias, J. D.; et al. Reimagining high-throughput profiling of reactive cysteines for cell-based screening of large electrophile libraries. *Nat. Biotechnol.* **2021**, *39*, 630−641.
(25) Backus, K. M.; Correia, B. E.; Lum, K. M.; Forli, S.; Horning, B. D.; González-Páez, G. E.; Chatterjee, S.; Lanning, B. R.; Teijaro, J. R.; Olson, A. J.; Wolan, D. W.; Cravatt, B. F. Proteome-wide covalent ligand discovery in native biological systems. *Nature* **2016**, *534*, 570−574.
(26) Bar-Peled, L.; Kemper, E. K.; Suciu, R. M.; Vinogradova, E. V.; Backus, K. M.; Horning, B. D.; Paul, T. A.; Ichu, T. A.; Svensson, R. U.; Olucha, J.; et al. Chemical Proteomics Identifies Druggable Vulnerabilities in a Genetically Defined Cancer. *Cell* **2017**, *171*, 696.
(27) Roberts, A. M.; Miyamoto, D. K.; Huffman, T. R.; Bateman, L. A.; Ives, A. N.; Akopian, D.; Heslin, M. J.; Contreras, C. M.; Rape, M.; Skibola, C. F.; et al. Chemoproteomic Screening of Covalent Ligands Reveals UBA5 As a Novel Pancreatic Cancer Target. *ACS Chem. Biol.* **2017**, *12*, 899−904.
(28) Chung, C. Y.-S.; Shin, H. R.; Berdan, C. A.; Ford, B.; Ward, C. C.; Olzmann, J. A.; Zoncu, R.; Nomura, D. K. Covalent targeting of the vacuolar H(+)-ATPase activates autophagy via mTORC1 inhibition. *Nat. Chem. Biol.* **2019**, *15*, 776−785.

https://doi.org/10.1021/acschembio.1c00824
ACS Chem. Biol. XXXX, XXX, XXX−XXX

(29) Grossman, E. A.; Ward, C. C.; Spradlin, J. N.; Bateman, L. A.; Huffman, T. R.; Miyamoto, D. K.; Kleinman, J. I.; Nomura, D. K. Covalent Ligand Discovery against Druggable Hotspots Targeted by Anti-cancer Natural Products. *Cell Chem. Biol.* **2017**, *24*, 1368.
(30) Vinogradova, E. V.; Zhang, X.; Remillard, D.; Lazar, D. C.; Suciu, R. M.; Wang, Y.; Bianco, G.; Yamashita, Y.; Crowley, V. M.; Schafroth, M. A.; Yokoyama, M.; Konrad, D. B.; Lum, K. M.; Simon, G. M.; Kemper, E. K.; Lazear, M. R.; Yin, S.; Blewett, M. M.; Dix, M. M.; Nguyen, N.; Shokhirev, M. N.; Chin, E. N.; Lairson, L. L.; Melillo, B.; Schreiber, S. L.; Forli, S.; Teijaro, J. R.; Cravatt, B. F. An Activity-Guided Map of Electrophile-Cysteine Interactions in Primary Human T Cells. *Cell* **2020**, *182*, 1009.
(31) Crowley, V. M.; Thielert, M.; Cravatt, B. F. Functionalized Scout Fragments for Site-Specific Covalent Ligand Discovery and Optimization. *ACS Cent. Sci.* **2021**, *7*, 613−623.
(32) Brighty, G. J.; Botham, R. C.; Li, S.; Nelson, L.; Mortenson, D. E.; Li, G.; Morisseau, C.; Wang, H.; Hammock, B. D.; Sharpless, K. B.; et al. Using sulfuramidimidoyl fluorides that undergo sulfur(VI) fluoride exchange for inverse drug discovery. *Nat. Chem.* **2020**, *12*, 906−913.
(33) Ábrányi-Balogh, P.; Petri, L.; Imre, T.; Szijj, P.; Scarpino, A.; Hrast, M.; Mitrović, A.; Fonović, U. P.; Németh, K.; Barreteau, H.; Roper, D. I.; Korvati, K.; Ferenczy, G. G.; Kos, J.; Ilas, J.; Gobec, S.; Keseru, G. M. A road map for prioritizing warheads for cysteine targeting covalent inhibitors. *Eur. J. Med. Chem.* **2018**, *160*, 94−107.
(34) Takaya, J.; Mio, K.; Shiraishi, T.; Kurokawa, T.; Otsuka, S.; Mori, Y.; Uesugi, M. A Potent and Site-Selective Agonist of TRPA1. *J. Am. Chem. Soc.* **2015**, *137*, 15859−15864.
(35) Chen, Y. C.; Backus, K. M.; Merkulova, M.; Yang, C.; Brown, D.; Cravatt, B. F.; Zhang, C. Covalent Modulators of the Vacuolar ATPase. *J. Am. Chem. Soc.* **2017**, *139*, 639−642.
(36) Yu, Y.; Hamza, A.; Zhang, T.; Gu, M.; Zou, P.; Newman, B.; Li, Y.; Gunatilaka, A. A. L.; Zhan, C. G.; Sun, D. Withaferin A targets heat shock protein 90 in pancreatic cancer cells. *Biochem. Pharmacol.* **2010**, *79*, 542−551.
(37) Chen, Y.; Zhu, J. Y.; Hong, K. H.; Mikles, D. C.; Georg, G. I.; Goldstein, A. S.; Amory, J. K.; Schönbrunn, E. Structural Basis of ALDH1A2 Inhibition by Irreversible and Reversible Small Molecule Inhibitors. *ACS Chem. Biol.* **2018**, *13*, 582−590.
(38) Low, W. K.; Dang, Y.; Schneider-Poetsch, T.; Shi, Z.; Choi, N. S.; Merrick, W. C.; Romo, D.; Liu, J. O. Inhibition of eukaryotic translation initiation by the marine natural product pateamine A. *Mol. Cell* **2005**, *20*, 709−722.
(39) Cole, K. S.; Grandjean, J. M. D.; Chen, K.; Witt, C. H.; O'Day, J.; Shoulders, M. D.; Wiseman, R. L.; Weerapana, E. Characterization of an A-Site Selective Protein Disulfide Isomerase A1 Inhibitor. *Biochemistry* **2018**, *57*, 2035−2043.
(40) Yun, J.; Mullarky, E.; Lu, C.; Bosch, K. N.; Kavalier, A.; Rivera, K.; Roper, J.; Chio, I. I.; Giannopoulou, E. G.; Rago, C.; et al. Vitamin C selectively kills KRAS and BRAF mutant colorectal cancer cells by targeting GAPDH. *Science* **2015**, *350*, 1391−1396.
(41) Kunjithapatham, R.; Ganapathy-Kanniappan, S. GAPDH with NAD(+)-binding site mutation competitively inhibits the wild-type and affects glucose metabolism in cancer. *Biochim. Biophys. Acta Gen. Subj.* **2018**, *1862*, 2555−2563.
(42) Boroughs, L. K.; DeBerardinis, R. J. Metabolic pathways promoting cancer cell survival and growth. *Nat. Cell Biol.* **2015**, *17*, 351−359.
(43) Wagener, J.; Schneider, J. J.; Baxmann, S.; Kalbacher, H.; Borelli, C.; Nuding, S.; Küchler, R.; Wehkamp, J.; Kaeser, M. D.; Mailänder-Sanchez, D.; Braundorf, C.; Hube, B.; Schild, L.; Forssmann, W.-G.; Korting, H.-C.; Liepke, C.; Schaller, M. A peptide derived from the highly conserved protein GAPDH is involved in tissue protection by different antifungal strategies and epithelial immunomodulation. *J. Invest. Dermatol.* **2013**, *133*, 144−153.
(44) Nakano, T.; Goto, S.; Takaoka, Y.; Tseng, H. P.; Fujimura, T.; Kawamoto, S.; Ono, K.; Chen, C. L. A novel moonlight function of glyceraldehyde-3-phosphate dehydrogenase (GAPDH) for immuno-modulation. *BioFactors* **2018**, *44*, 597−608.
(45) Kornberg, M. D.; Bhargava, P.; Kim, P. M.; Putluri, V.; Snowman, A. M.; Putluri, N.; Calabresi, P. A.; Snyder, S. H. Dimethyl fumarate targets GAPDH and aerobic glycolysis to modulate immunity. *Science* **2018**, *360*, 449−453.
(46) Colell, A.; Ricci, J. E.; Tait, S.; Milasta, S.; Maurer, U.; Bouchier-Hayes, L.; Fitzgerald, P.; Guio-Carrion, A.; Waterhouse, N. J.; Li, C. W.; Mari, B.; Barbry, P.; Newmeyer, D. D.; Beere, H. M.; Green, D. R. GAPDH and autophagy preserve survival after apoptotic cytochrome c release in the absence of caspase activation. *Cell* **2007**, *129*, 983−997.
(47) Wang, H.; Wang, M.; Yang, X.; Xu, X.; Hao, Q.; Yan, A.; Hu, M.; Lobinski, R.; Li, H.; Sun, H. Antimicrobial silver targets glyceraldehyde-3-phosphate dehydrogenase in glycolysis of E. coli. *Chem. Sci.* **2019**, *10*, 7193−7199.
(48) Butterfield, D. A.; Hardas, S. S.; Lange, M. L. B. Oxidatively modified glyceraldehyde-3-phosphate dehydrogenase (GAPDH) and Alzheimer's disease: many pathways to neurodegeneration. *J. Alzheimers Dis.* **2010**, *20*, 369−393.
(49) Aronov, A. M.; Verlinde, C. L. M. J.; Hol, W. G. J.; Gelb, M. H. Selective tight binding inhibitors of trypanosomal glyceraldehyde-3-phosphate dehydrogenase via structure-based drug design. *J. Med. Chem.* **1998**, *41*, 4790−4799.
(50) Bruno, S.; Pinto, A.; Paredi, G.; Tamborini, L.; De Micheli, C.; La Pietra, V.; Marinelli, L.; Novellino, E.; Conti, P.; Mozzarelli, A. Discovery of covalent inhibitors of glyceraldehyde-3-phosphate dehydrogenase, a target for the treatment of malaria. *J. Med. Chem.* **2014**, *57*, 7465−7471.
(51) Galbiati, A.; Zana, A.; Conti, P. Covalent inhibitors of GAPDH: From unspecific warheads to selective compounds. *Eur. J. Med. Chem.* **2020**, *207*, 112740.
(52) Kok, B. P.; Ghimire, S.; Kim, W.; Chatterjee, S.; Johns, T.; Kitamura, S.; Eberhardt, J.; Ogasawara, D.; Xu, J.; Sukiasyan, A.; et al. Discovery of small-molecule enzyme activators by activity-based protein profiling. *Nat. Chem. Biol.* **2020**, *16*, 997−1005.

https://doi.org/10.1021/acschembio.1c00824
ACS Chem. Biol. XXXX, XXX, XXX−XXX